Attenuation of longitudinal-acoustic phonons in amorphous SiO_2 at frequencies up to 440 GHz

T. C. Zhu, H. J. Maris, and J. Tauc
Department of Physics and Division of Engineering, Brown University, Providence, Rhode Island 02912
(Received 14 February 1991)

We report measurements of the attenuation of longitudinal-acoustic phonons in amorphous SiO_2 for frequencies between 76 and 440 GHz, and in the temperature range 80–300 K. The samples are chemical-vapor-deposited films grown on tungsten substrates, and the phonons are generated and detected using picosecond optical techniques. The phonon attenuation is found to depend only weakly on temperature. In the upper part of the frequency range, there is some evidence that the frequency dependence is faster than quadratic, thus indicating that the attenuation cannot be explained by classical relaxation theory. A discussion of the relation between these results and the analysis of thermal-conductivity measurements is given.

I. INTRODUCTION

Despite much work the thermal and acoustic properties of amorphous materials remain imperfectly understood. Experiments have shown that[1] while the behavior of amorphous and crystalline materials are very different, the properties of a wide range of different amorphous solids are surprisingly similar. These properties include a specific heat C that varies linearly with temperature below about 1 K, an anomalously large T^3 term in C at higher temperatures,[2] a thermal conductivity κ varying approximately as T^2 below 1 K, and a plateau in $\kappa(T)$ (i.e., a nearly temperature-independent region) at temperatures between roughly 2 and 10 K. The ultrasonic attenuation is much larger than in crystals, and has a complicated dependence on temperature, sound amplitude, and frequency.[3]

Even at the phenomenological level, it is only below 1 K that these properties of amorphous materials are understood. In this temperature range the specific heat, thermal conductivity, and ultrasonic attenuation can all be understood[4] by the two-level-system model (TLS) introduced by Phillips[5] and by Anderson, Halperin, and Varma.[6] Despite much experimental work the nature of the TLS defects has not been determined.[7] At higher temperatures, there is no generally accepted explanation of the T^3 term in the specific heat or of the temperature dependence of the thermal conductivity. If it is assumed that heat in glasses is carried by phonons, then the thermal conductivity should be given by the kinetic formula

$$\kappa(T)=\tfrac{1}{3}\int_0^{\omega_D} C(\omega,T)\Lambda(\omega,T)v\,d\omega\ , \tag{1}$$

where $C(\omega,T)$ is the contribution to the specific heat per unit volume from phonons of angular frequency ω, $\Lambda(\omega,T)$ is the mean free path of these phonons, and v is their velocity.[8] From the single experimental quantity $\kappa(T)$ it is clearly impossible to determine uniquely the dependence of Λ on the two variables ω and T. If one assumes, however, that Λ is primarily a function of frequency (i.e., that the T dependence of Λ can be ignored), then a reasonably definite estimate of the form of Λ required to give the correct $\kappa(T)$ can be made.[9] For fused quartz this is shown[10] in Fig. 1. At a critical frequency ν_c, which for a-SiO_2 is estimated to be about 100 GHz, Λ begins to decrease very rapidly, and over a narrow frequency range falls to a value of about 10 Å. This sharp drop in Λ is necessary to give the plateau in $\kappa(T)$.

The frequency dependence of the mean free path could be quite different if Λ has a significant dependence on T. There are a few experiments that bear on this issue, but at the present time these do not provide a complete picture. It is possible to use the tunnel-junction technique[11–16] to make measurements up to several hundred GHz at low temperature, typically $T \leq 2$ K. Data have been obtained by several groups, but there are some important differences in the results obtained, as we will discuss later. At higher temperatures, where junctions can-

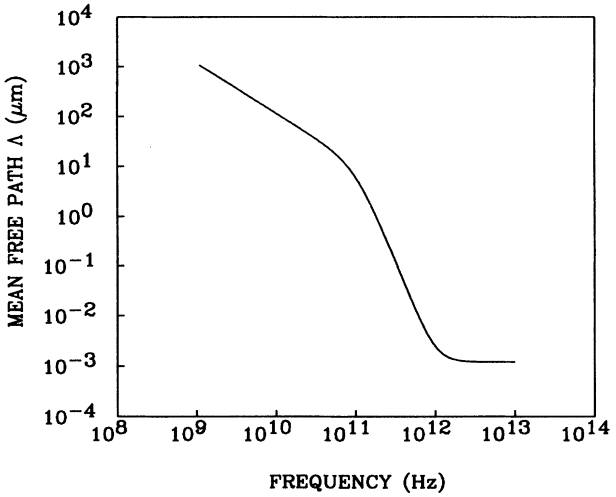

FIG. 1. Estimated frequency dependence of the phonon mean free path based on an analysis of the thermal conductivity κ. The fit is taken from Ref. 10.

not be used, the highest-frequency measurements[17] have been made by Brillouin scattering and are around 30 GHz. We have made preliminary reports[18,19] of measurements obtained at higher frequencies using a new method based on picosecond optics techniques. In this paper we describe the results of a more extensive set of measurements that cover the temperature range 80–300 K and extend in frequency up to 440 GHz. We describe the experimental method in the next section, and in Sec. III present the results and discuss uncertainties associated with this type of measurement. In Sec. IV we discuss the relation of these results to other probes of the phonon mean free path in glasses, including thermal conductivity and tunnel-junction measurements.

II. EXPERIMENT

A. Apparatus

The experimental arrangement is shown schematically in Fig. 2. The a-SiO_2 sample was a thin film deposited onto a (100) single-crystal tungsten substrate. An aluminium film for use as a transducer was evaporated on top of the SiO_2. To generate a sound pulse a short light pulse (the "pump" pulse) was focused onto a small area of the Al film. The increase in temperature of the Al caused it to expand, thereby launching a strain pulse into the sample. This strain propagated through the SiO_2 sample and was then partially reflected at the SiO_2-W interface. On returning to the Al transducer the strain caused a small change in the optical reflectivity. This change was measured by means of a time-delayed probe pulse. To make the measurements the time dependence of the reflectivity change $\Delta R(t)$ was measured by sweeping the time delay of the probe. The magnitude of ΔR was typically of the order of 10^{-5}, and so it was necessary to use modulation techniques together with a large amount of signal averaging to obtain accurate measurements. Some typical data are shown in Fig. 3. These are for a 750-Å film of SiO_2 with a 130-Å Al transducer.

In these experiments we used[20] a Nd:YAG (yttrium aluminum garnet) mode-locked IR laser, which, after frequency doubling and pulse compression, synchronously pumped a dye laser to produce 0.5-nJ pulses at 585 nm.

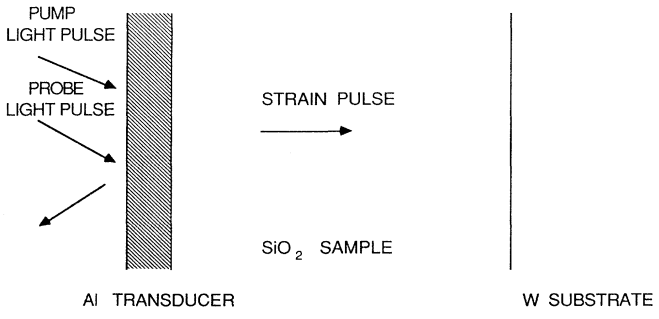

FIG. 2. Schematic diagram of the experiment.

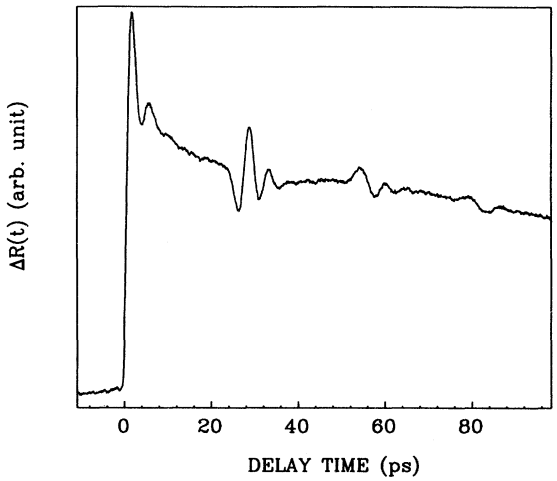

FIG. 3. Experimental data (reflectivity change ΔR as a function of time) for a 750-Å SiO_2 film at 160 K.

The pulse duration τ_0 was typically 0.5 psec. The pump and probe beams were focused to a diameter of ~ 20 μm on the transducer surface, and the energy per pulse in these beams was typically 0.1 and 0.01 nJ, respectively. From the calculated heat capacity of the illuminated area of the Al film we could find the temperature jump produced by each pump pulse. This was about 1 K at an ambient temperature of 300 K, rising to 3 K at 80 K. In addition, the pump and probe beams produced a steady-state temperature increase of the Al relative to the temperature of the W substrate. To make an estimate of this we assumed that the SiO_2 films had the same thermal conductivity as bulk a-SiO_2. This temperature increase is proportional to the sample thickness, and is larger at lower ambient temperatures. However, even for a 5000-Å sample at 80 K it is only 1.5 K. Thus, under the conditions of the experiment both the transient and steady-state heating of sample by the laser were small effects.

B. Sample and transducer

The a-SiO_2 film was grown on the W substrate by chemical-vapor deposition (CVD). We chose this method because other studies[21] have shown that films prepared in this way have properties close to those of bulk SiO_2. The substrate temperature was 720 K, and the flow rates of the oxygen, nitrogen, and silane were controlled to achieve a growth rate of around 2 Å sec^{-1}. The film thickness was determined by means of an ellipsometer, and it was found that the thickness variation over the film area (~ 0.8 cm^2) was less than 10%. The ellipsometer measurement gave a value of 1.46 for the refractive index at a wavelength of 633 nm, which agrees with the refractive index of bulk SiO_2.[22]

Tungsten was chosen for the substrate material because of its very high acoustic impedance. This results in a large reflection coefficient of the strain pulse at the SiO_2-substrate interface. Before deposition of the SiO_2 the W

substrates[23] were mechanically polished and, in some cases, given a further electromechanical polish.[24]

The Al transducer film had a typical thickness of 130 Å, and was evaporated onto the SiO_2. The growth rate was 2 Å sec^{-1} in a vacuum of $\sim 10^{-6}$ Torr. Aluminium was chosen as the transducer material because it has nearly the same acoustic impedance as SiO_2. Consequently, there should be only a small acoustic reflection at this interface. In addition, Al has the advantage of high optical absorption, which means that even a 130-Å film can absorb essentially all the light in the pump pulse.

C. Analysis of data

The measured results for $\Delta R(t)$ show the acoustic echoes superposed on a smoothly decaying background (see Fig. 3). This background arises because there is a contribution to ΔR from the change in temperature of the Al films. This temperature relaxes as heat flows from the Al through the SiO_2 into the W substrate. In the first step in the data analysis we made a fit to this background and then subtracted it from the raw data. This left the data in the form of a series of separated echoes with a background between them, which was zero apart from random noise.

The Al film, when suddenly heated by the pump pulse, produces a strain pulse in the SiO_2 with a complex shape, as discussed below. At the SiO_2-W interface this pulse is reflected with amplitude reduced by a factor r_{FS}, and with no change in shape. When the pulse returns to the Al it has a shape $\eta(z,t)$ and produces a change in reflectivity which can be written as

$$\Delta R(t)=\int_0^d f(z)\eta(z,t)\,dz \ , \tag{2}$$

where $\eta(z,t)$ is the strain at depth z into the film, and d is the film thickness. The sensitivity function $f(z)$ can be calculated from the optical constants of Al, and their derivatives with respect to strain (see details in the Appendix). This result assumes that the main contribution to $\Delta R(t)$ comes from the strain-induced changes in the optical properties of the Al; if sufficient light penetrates the Al and enters the SiO_2 there can be a contribution to ΔR from the time-varying strain in the sample itself. To predict the shape $\Delta R_1(t)$ of the echo it is necessary to calculate not only the shape of the strain pulse as it propagates through the SiO_2, but also how this pulse is modified when in the Al due to reflection at both surfaces of the Al film. These reflections also mean that after reflection at the Al the strain pulse $\eta_2(z,t)$ returning into the SiO_2 has a different shape from the pulse $\eta_1(z,t)$ as initially launched. Thus, calculating the shape of the echoes ΔR_1, ΔR_2 is not simple.

Fortunately, this calculation does not have to be done in order to find the attenuation. Let us write the returning strain pulse $\eta_1(z,t)$ in terms of its Fourier components $\eta_1(\omega)$:

$$\eta_1(z,t)=\int_{-\infty}^{\infty} d\omega\,\eta_1(\omega)e^{i\omega(t+z/v)} \ . \tag{3}$$

Each Fourier component will make a contribution to $\Delta R_1(t)$. Thus we must have

$$\Delta R_1(\omega)=F(\omega)\eta_1(\omega) \ , \tag{4}$$

where $F(\omega)$ can, in principle, be calculated from $f(z)$. For the second echo

$$\Delta R_2(\omega)=F(\omega)\eta_2(\omega) \ . \tag{5}$$

If we assume there is no acoustic attenuation in the transducer film then it must be true that

$$\eta_2(\omega)=\eta_1(\omega)r_{FS}e^{i\phi(\omega)}e^{-2\alpha(\omega)d_s} \ , \tag{6}$$

where $\phi(\omega)$ is a phase shift applied to the Fourier component ω each time the strain pulse is reflected from the transducer, d_s is the thickness of the SiO_2 sample and $\alpha(\omega)$ is the attenuation per unit distance in the sample film. Thus, from (4)–(6) we have

$$\alpha(\omega)=\frac{1}{2d_s}\ln|\Delta R_1(\omega)r_{FS}/\Delta R_2(\omega)| \ . \tag{7}$$

To calculate r_{FS} we have used acoustic mismatch theory. For the density and sound velocity of the SiO_2 we took the values[25] for bulk SiO_2, i.e., $\rho=2.2$ g/cm^3 and $v=59$ Å/ps, and for W we used the density 19.35 g/cm^3 and the sound velocity 52 Å/ps corresponding to the longitudinal velocity in the (100) direction. These parameters give $r_{FS}=0.77$.

Some typical results for $\Delta R_n(\omega)$ $(n=1,2,3)$ are shown in Fig. 4. These are for a film of thickness 750 Å at 160 K. For a given film thickness such data provide a means to calculate the attenuation over a certain range of frequency. At low frequency the attenuation α becomes small, and so $|\Delta R_1 r_{FS}/\Delta R_2|$ is close to 1. Then the small uncertainty that must exist in the value of r_{FS} (due to lack of precise knowledge of the density and sound velocity in the film, for example) gives a large error in α. At high frequency the method is limited by the rapid decrease of $\Delta R_2(\omega)$, which eventually falls to a value comparable to the noise. In a typical case, data from a single

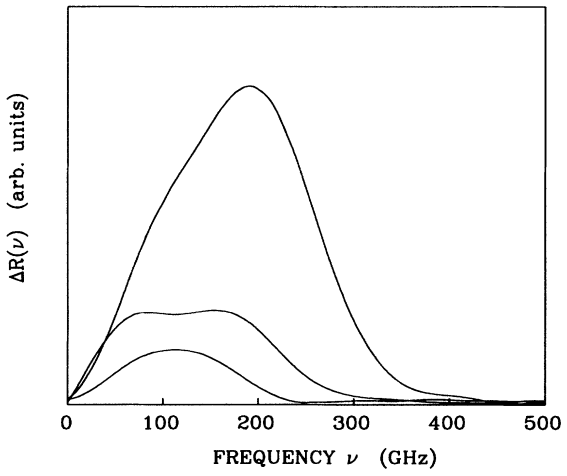

FIG. 4. Fourier transforms of the first three echoes in a 750-Å SiO_2 film at 160 K.

sample thickness could be used to find the attenuation over a frequency range of about a factor of 2. To measure α over a broad frequency range we therefore used a series of samples with different thicknesses.

As an overall check on our understanding of the physical processes involved in the measurement, we have calculated the expected shape $\Delta R_1(t)$ of the first acoustic echo. To do this it is necessary to estimate the strain $\eta_1(z,t)$ produced in the transducer by the first acoustic echo and the sensitivity function $f(z)$. This calculation is described in the Appendix, and the sensitivity function is shown in Fig. 5 (a). This result is subject to uncertainty because some of the key quantities required to find $f(z)$ are not known (see discussion in the Appendix), and the thickness of the Al transducer is treated as an adjustable parameter. Nevertheless, the final result for the shape of the first echo [Fig. 5(b)] is in reasonable agreement with experiment.

To determine the thickness d_2 of the sample the following method was used. The time T between echoes is the time for the sound to make a round trip through the sample and the transducer. Thus,

$$d_s = v_s \left[\frac{T}{2} - \frac{d}{v_{\mathrm{Al}}} \right] . \tag{8}$$

We could determine an approximate value for the thickness of the Al film by varying the assumed thickness to obtain a best fit to the echo shape by the method just described. To within experimental error the result obtained was in agreement with the thickness independently measured by means of a quartz crystal-thickness monitor. To determine d_s from Eq. (8) we then used the experimentally measured value of T, together with the literature values for the sound velocities in bulk Al and SiO_2.[25] The final values obtained for d_s were within 10% of direct ellipsometric measurements, except for the very thin films for which the errors in the ellipsometric technique became larger.

III. RESULTS

Data were taken on a total of nine SiO_2 samples. Results for the attenuation as a function of temperature are shown in Fig. 6. In order to make a later comparison with the phonon mean-free-path data shown in Fig. 1 we have plotted the rate of attenuation per unit distance of the *energy* in the strain pulse, i.e., twice the quantity $\alpha(\omega)$ defined in Eq. (7). The solid curves are given as a guide to the eye. To within the experimental error the attenuation is found to be temperature independent over the

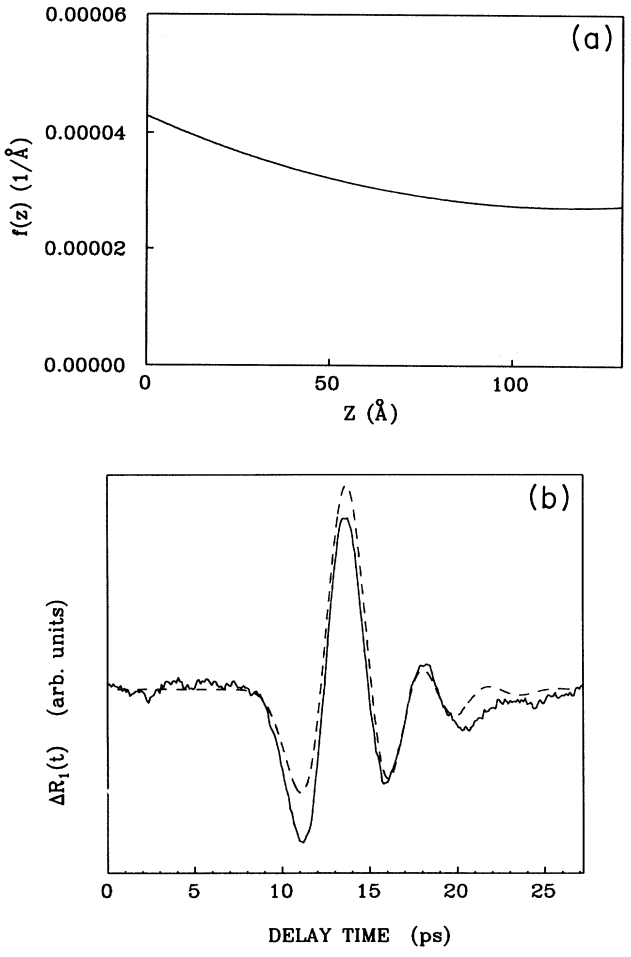

FIG. 5. (a) Sensitivity functions $f(z)$ as a function of depth z into the transducer film according to the theory described in the Appendix. $\partial\epsilon_1/\partial\eta_{zz}$ has been arbitrarily set equal to -1. Calculation is for an Al film of thickness 130 Å. (b) Comparison of the shape of the first acoustic echo with theory. Experimental result is solid curve; theory is dashed curve.

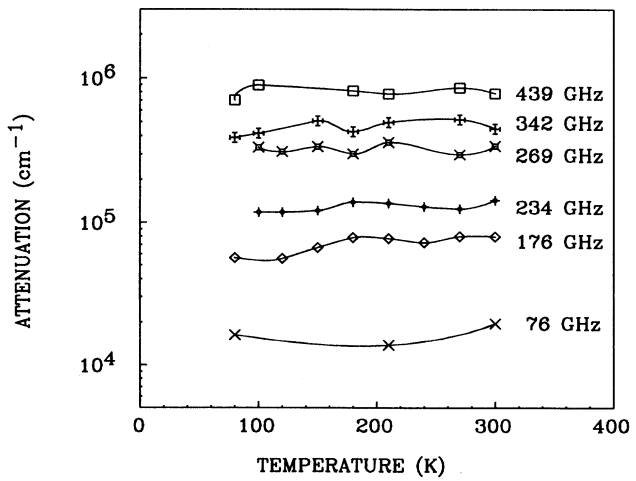

FIG. 6. Phonon attenuation in SiO_2 as a function of temperature. The quantity plotted is the rate of attenuation of the energy of the sound wave with distance. The 76-GHz data are from the 5800-Å sample, the 176- and 236-GHz data are from the 984-Å sample, and the 269-, 342-, and 439-GHz data from the 280-Å sample.

range studied (80–300 K). The attenuation at 76 GHz is taken from a sample 5800 Å thick, the attenuation between 176 and 234 GHz from a 984-Å sample, and the attenuation between 269 and 439 GHz from a 280-Å sample. As described in Sec. II A, we have carefully examined the effect of laser heating to ensure that the temperature is correct.

The attenuation as a function of frequency at several temperatures between 80 and 300 K is shown in Fig. 7. As in Fig. 6 the energy attenuation is plotted. The data that are shown were obtained from the same three samples used to obtain the results of Fig. 6. For each of the samples we have plotted data over a broad frequency range so that the data overlap in frequency to some extent. The 280-Å sample gives data in the frequency range 240–440 GHz, the 984-Å sample from 140 to 300 GHz, and the 5800-Å sample from 30 to 100 GHz. Taken over the entire frequency range studied the attenuation varies roughly quadratically with frequency. However, one can see from Fig. 7 that the results suggest that the frequency dependence may, in fact, be slower than quadratic in the lower part of the frequency range and faster than quadratic at high frequencies. We will discuss this point in the next section.

One possible source of error in the experiment comes from attenuation in the Al film. We have calculated the attenuation to be expected because of the interaction of the sound wave with the conduction electrons using Pippard theory.[26] In the frequency range studied the attenuation is negligible. More serious errors may arise from the acoustic quality of the interfaces in the structure. One can consider at least three possible effects. (a) If the bonding between the SiO_2 and W is poor, r_{FS} should be larger than calculated by the acoustic mismatch theory. This error means that our measured attenuation values are too low. (b) A poor bond between the Al and the SiO_2 does not affect the results, provided there is no dissipation (acoustic loss) at this interface. Poor bonding at this interface shows up in ringing of the transducer, and an example is shown in Fig. 8. Transducers showing this behavior were not used. (c) If the bond between the transducer and the film produces acoustic loss the measured values of attenuation are too high. With a single sample (a) and (c) cannot be detected. The only possible approach is to study a series of samples of different thickness, and to see if the results are consistent. Analysis of the data taken on the six other samples gives values for the attenuation which are, in general, consistent with the data shown in Figs. 6 and 7.

The roughness of the substrate surface can, in principle, lead to a spurious attenuation which is hard to eliminate even by measurements on a series of samples of different thickness. We expect that, to some extent, the area of the surface illuminated by the pump and probe beams will be corrugated as shown qualitatively in Fig. 9. It is reasonable to expect that the thickness d_s of the sample film measured in the direction normal to the *average* orientation of the substrate surface will be nearly constant. But this means that the actual acoustic path d_{ac} will be different for different points on the sample (see Fig. 9). This variation in acoustic path is proportional to the thickness of the sample, and hence gives an acoustic loss (due to different parts of the wave front becoming out of phase) which increases with increasing film thickness. Thus, one cannot eliminate this spurious source of attenuation even by measurements on a series of samples of different thickness. The best evidence that we have against this being a large (or dominant) effect is the observation that we find similar values for the attenuation on

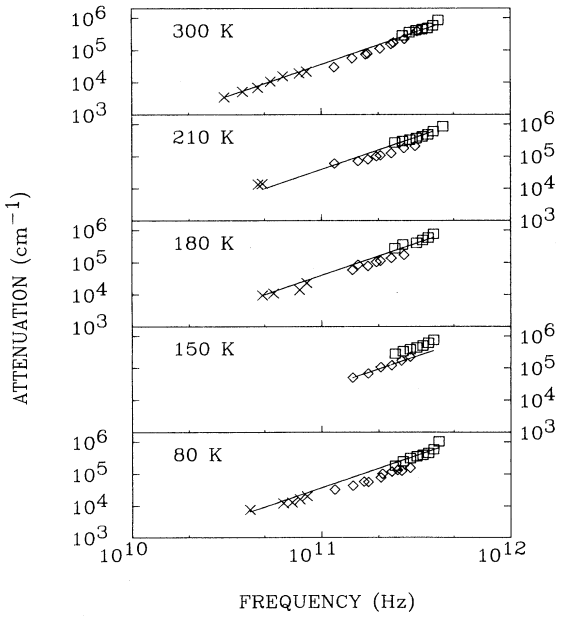

FIG. 7. Phonon attenuation in SiO_2 as a function of phonon frequency. The quantity plotted is the rate of attenuation of the energy of the sound wave with distance. ×, 5800-Å SiO_2 sample; ◇, 984-Å SiO_2; and □, 280-Å SiO_2 sample. The solid lines are fits with f^2. See text for more details.

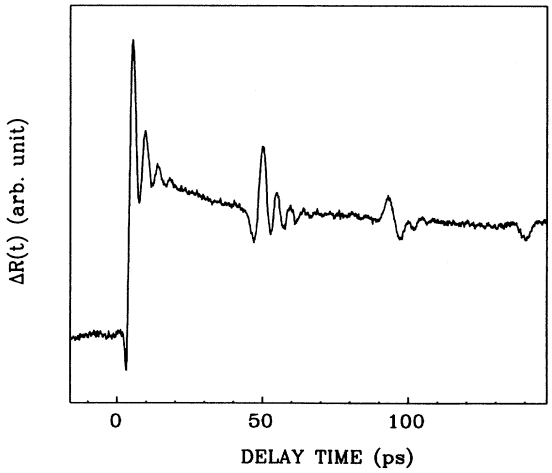

FIG. 8. Experimental data from a sample with poor bonding of the Al transducer to the SiO_2 sample film.

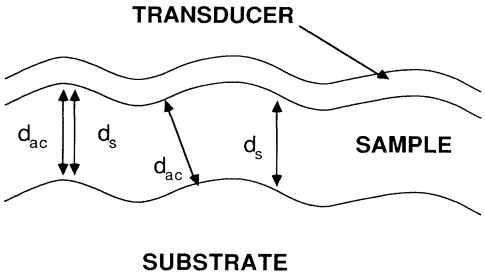

FIG. 9. Corrugation of the substrate surface causes the acoustic path d_{ac} to vary across the sample, even though the film thickness d_s measured normal to the substrate is constant.

samples that have received somewhat different polishing treatments.

IV. DISCUSSION

We can compare our results with other data to try to get an overview of the dependence of the phonon mean free path Λ on frequency and temperature. Several groups have performed experiments to study phonon propagation in glasses using tunnel-junction techniques. The measurements lie in a range of frequency that overlaps ours, but the temperature range is usually limited to a fairly small region around 1 K. It should be noted that the tunnel-junction experiments are to a good approximation measuring the mean free path of transverse phonons, whereas we have measured longitudinal phonons. The first experiments were performed by Dietsche and Kinder[11] with electron-beam-evaporated SiO_2 sample films. They made measurements from around 100 GHz up to 290 GHz and found a mean free path varying as $\nu^{-2.9}$ (ν=phonon frequency). At 290 GHz Λ was found to be about 5000 Å. Within experimental error no temperature dependence was detected, but this was based only upon data taken at 1.05 and 1.25 K. Wolter and Horstman[12] studied films prepared by the oxidation of a silicon surface in a similar temperature range to that investigated by Dietsche and Kinder and obtained much larger values for Λ. Their conclusion was that at 300 GHz Λ was larger that 4 μm. No significant temperature dependence was detected between 45 and 450 mK. Further measurements in the same frequency range were made by Long and co-workers[14]. Radio-frequency sputtered films were used and at 240 GHz the measured value of Λ was found to be 2.2 μm, varying roughly as ν^{-6}.

Quantitative measurements at higher frequencies are not available, but there are at least two experiments that set approximate lower limits on the phonon mean free path. In an experiment by Rothenfusser, Dietsche, and Kinder[16] acoustic standing-wave resonances were observed in a 530-Å SiO_2 film grown by thermal oxidation. The results implied that the value of Λ at 400 GHz was at least 1500 Å. In a somewhat similar experiment Koblinger *et al.*[3] studied phonon transmission through amorphous Si-SiO_2 multilayer structures and were able to detect the stopbands of the periodic structure. The total thickness of SiO_2 was 490 Å and it was possible to see some structure in the transmission due to the stopbands even up to 700 GHz. They did not make an estimate of the limit that this imposes on the value of Λ, but it seems unlikely that one could see this type of structure if Λ were less than the total thickness of the SiO_2.

The values of Λ obtained by the tunnel-junction method are much larger that the results we have obtained at higher temperatures. At 300 GHz we obtain a value of Λ of 300 Å (roughly constant within our temperature range), whereas the tunnel-junction experiments just mentioned give Λ in the vicinity of 1 μm.

The estimate of the phonon mean free path obtained[10] from the thermal conductivity of bulk SiO_2 has already been shown in Fig. 1. This estimate gives a mean free path at 300 GHz of 1500 Å, i.e., about five times our result, whereas at 440 GHz the difference is reduced to a factor of 3.

Of course, these comparisons are all subject to the uncertainty of differences between samples. In addition, there could be a significantly different attenuation for longitudinal and transverse phonons. Nevertheless, taken as a whole the results from our experiments, together with the tunnel junction and thermal-conductivity data do suggest that for a given frequency the general trend is that

$$\Lambda_{TJ} > \Lambda_{TC} > \Lambda_{PU} , \tag{9}$$

where Λ_{TJ}, Λ_{TC}, and Λ_{PU} are the values of Λ measured by tunnel junctions, thermal conductivity, and picosecond ultrasonics, respectively. The tunnel-junction measurements are made at around 1 K. Thermal conductivity measures the average mean free path for phonons thermally excited at temperature T, i.e., phonons of typical frequency around $3k_BT/\hbar$ (k_B=Boltzmann's constant). Thus, when the thermal conductivity is analyzed to yield the frequency dependence of Λ one should consider that it gives for a particular frequency ω the mean free path at a temperature of about $\hbar\omega/3k_B$. Thus, in the frequency range where we have been comparing values of Λ (i.e., roughly 100–500 GHz) the effective temperature (2–8 K) for the Λ determined from thermal conductivity is higher than the temperature at which the tunnel-junction measurements were made. In turn, in this same frequency range the temperature for our ultrasonic measurements is higher than the thermal-conductivity effective temperature. Thus, taken together the three sets of data indicate that the mean free path has a significant temperature dependence.

Measurements at lower frequencies (in the vicinity of 30 GHz) by Vacher *et al.*[17] do give a mean free path that decreases substantially as the temperature is raised from helium temperatures up to 80 K, and then becoming essentially independent of temperature at higher temperatures. Thus, the present analysis suggests that this behavior persists at higher frequencies. Of course, it would be interesting to try to confirm this directly by extending the picosecond ultrasonic measurements to lower temperatures. Unfortunately, this is very hard to do because of

the heating of the sample by the laser pulse.

If it is true that Λ for a constant frequency decreases with increasing T, then to be consistent with the temperature dependence of the thermal conductivity it would be required that the rapid decrease in Λ in the frequency range $10^{11}-10^{12}$ be slower than indicated on Fig. 1. It must, nevertheless, still have a fairly rapid decrease with increasing frequency in order to be consistent with the experiments of Zaitlin and Anderson,[9] who studied the effect on the thermal conductivity of introducing into a glass sample a large number of small holes.

Finally, we make some comments about the possibility of interpreting the measured attenuation in terms of a relaxation theory. Ultrasonic attenuation data at lower frequencies in SiO_2 and other glasses have been analyzed in terms of different models of relaxing structural defects.[27] In these models it is assumed that some defects in the glass can make thermally activated transitions between two or more states. The temperature dependence of the attenuation is determined by the spectrum of the barrier heights and the separation in energy of the different states of the defects. In Fig. 10 we show the attenuation in SiO_2 over the frequency range from 660 KHz to 440 GHz. We have made this plot for 90 K because at this temperature a large amount of data exists over a broad frequency range.[28-32] One can see that, considering the variety of samples and techniques that were used in these measurements, the different measurements form a reasonably consistent pattern. According to a relaxation theory at any given temperature the frequency dependence of the phonon attenuation (or equivalently the inverse of the phonon mean free path) can be expressed as

$$\Lambda(\omega,T)=\int F(\tau,T)\frac{\omega^2\tau}{1+\omega^2\tau^2}d\tau\ , \tag{10}$$

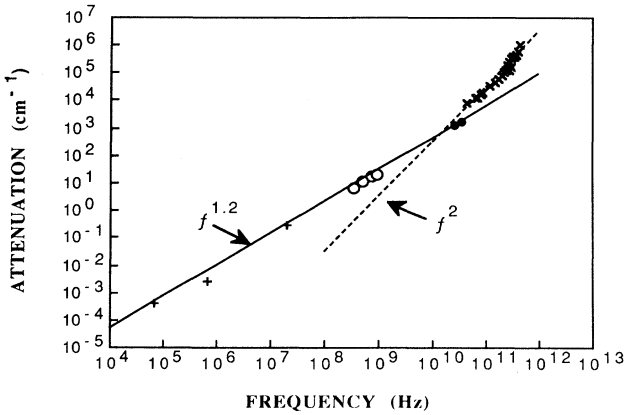

FIG. 10. Attenuation versus frequency in SiO_2 over a broad frequency range. The quantity plotted is the rate of attenuation of the energy of the sound wave with distance. The measurements of the present paper are denoted by $\times$. Lower-frequency data are taken from: (+) Ref. 30, (○) Ref. 32, (●) Ref. 28. The solid line is a fit of low-frequency data with $f^{1.2}$, the dashed line is a fit of our data with f^2.

where F describes the spectrum of relaxation times τ for the defects at temperature T. There are serious problems in explaining the measured mean free path in terms of any theory of this type. The first difficulty is that our attenuation data at the upper end of the frequency range have a frequency dependence that appears to be somewhat faster than quadratic. Regardless of the form of the function F, Eq. (10) always will give an attenuation that goes slower than quadratically, and hence cannot fit the data. The only way out of this difficulty is to argue that the accuracy of the data at high frequency is insufficient to justify the assertion that the frequency dependence is faster than quadratic. A second problem arises from the range of relaxation times that are required. The data extend up to a maximum frequency $\nu_{\max}$ of 440 GHz. To get a theoretical attenuation close to quadratic up to this frequency one needs there to be defects with relaxation times τ such that

$$\tau \ll \frac{1}{2\pi\nu_{\max}}\ . \tag{11}$$

Thus, one needs defects with τ much less than 3.6×10^{-13} sec. The relaxation time can be expressed as

$$\tau=\nu_{\text{attempt}}^{-1}\exp(U/k_BT)\ , \tag{12}$$

where ν_{attempt} is the frequency with which the defect attempts to go from one state to the other and U is the height of the barrier. Since ν_{attempt} must be in the THz range (i.e., comparable to the frequency of atomic vibrations) it is unlikely that Eq. (11) can be satisfied even if it is assumed that some barriers are extremely low. Consequently, it appears that a relaxation theory cannot explain the experimental results.

In the future we plan to make similar measurements in the same frequency range for other amorphous materials, including polymers. As part of this work we hope to look for correlations between acoustic and optical absorption as a function of material properties. A discussion of possible correlations of this type has been given by Strom.[33,34] It is interesting, for example, that in SiO_2 both the acoustic and optical absorption in the range 50–440 GHz vary nearly quadratically with frequency and are independent of temperature.[34]

ACKNOWLEDGMENTS

We thank T. R. Kirst for technical assistance, R. J. Stoner for discussions, and E. E. Crisman and C. Roberts for help in sample preparation. We thank W. Patterson, J. Rosenberg, and R. Paul for help in using the Brown microelectronic facilities. This work was supported by the DOE Grant No. DE-FG02-86ER45267.

APPENDIX

Let the dielectric constants of the Al and the SiO_2 be ϵ_1 and ϵ_2, respectively. We consider a probe light pulse with wave number k_0 at an angle of incidence θ polarized with its electric field parallel to the surface. The reflection and transmission coefficients across the interfaces between the air (medium 0), Al (medium 1), and SiO_2 (medium 2) are

most conveniently expressed in terms of the z components k_{0z}, k_{1z}, and k_{2z} of the light in the three media:

$$k_{0z}=k_0\cos\theta\ , \tag{A1}$$

$$k_{1z}=k_0\sqrt{\epsilon_1-\sin^2\theta}\ , \tag{A2}$$

$$k_{2z}=k_0\sqrt{\epsilon_2-\sin^2\theta}\ . \tag{A3}$$

Then, at the air-Al interface the reflection and transmission coefficients for the electric field amplitude are[35]

$$r_{01}=\frac{k_{0z}-k_{1z}}{k_{0z}+k_{1z}}\ , \tag{A4}$$

$$t_{01}=\frac{2k_{0z}}{k_{0z}+k_{1z}}\ . \tag{A5}$$

The amplitude reflection coefficient from the entire structure is [35]

$$r_0=\frac{r_{01}+r_{12}e^{2ik_{1z}d}}{1+r_{01}r_{12}e^{2ik_{1z}d}}\ . \tag{A6}$$

Suppose now that at a distance z into the Al film there is a thin layer of material of thickness δz whose dielectric constant has been changed by $\Delta\epsilon_1$. A wave of amplitude E_0 incident on this layer gives a reflected wave with amplitude $E_0 r'$, and a transmitted wave of amplitude $E_0(1+r')$. It is straightforward to show that

$$r'=\frac{ik_0^2}{2k_{1z}}\Delta\epsilon_1\delta z\ . \tag{A7}$$

Now consider the reflection coefficient of light from the Al-SiO_2 structure, allowing for the layer of material in the Al of changed dielectric constant. We calculate this by summing up all possible multiple reflections, subject to the restriction that only one reflection at the layer δz is allowed. The result is that the reflection coefficient becomes $r_0+\Delta r$, where

$$\Delta r=\frac{t_{01}t_{10}e^{2ik_{1z}z}(1+r_{12}e^{2ik_{1z}(d-z)})^2}{(1+r_{01}r_{12}e^{2ik_{1z}d})^2}\frac{ik_0^2\Delta\epsilon_1\delta z}{2k_{1z}}\ . \tag{A8}$$

In deriving this result it is important to allow for the fact that the layer modifies the wave transmitted through it, as well as generating a reflection. The change in the reflected intensity is then

$$\Delta R=|r_0+\Delta r|^2-|r_0|^2=2\,\mathrm{Re}(r_0^*\Delta r)\ , \tag{A9}$$

correct to first order in $\Delta\epsilon_1$. We can express $\Delta\epsilon_1$ as

$$\Delta\epsilon_1=\frac{\partial\epsilon_1}{\partial\eta_{zz}}\eta_{zz}\ . \tag{A10}$$

Then using (A6), (A8), (A10) and comparing with (2) we obtain, for the sensitivity function,

$$f(z)=-Rk_0^2\,\mathrm{Im}\left[\frac{t_{01}t_{10}e^{2ik_{1z}a}}{k_{1z}}\frac{(1+r_{12}e^{2ik_{1z}(d-z)})^2}{(r_{01}+r_{12}e^{2ik_{1z}d})}\times\frac{\partial\epsilon_1/\partial\eta_{zz}}{(1+r_{01}r_{12}e^{2ik_{1z}d})}\right]\ , \tag{A11}$$

where R is the intensity reflection coefficient $|r_0|^2$. For Al at 590-nm wavelength[36] $\epsilon_1=-48.8+16.4i$, and for SiO_2 (Ref. 22) $n_2=1.46$. Because the real part of ϵ_1 is much larger than the imaginary part we have approximated $\partial\epsilon_1/\partial\eta_{zz}$ in (A11) as a purely real quantity, assumed to be negative. This then gives $F(z)$ varying with z as shown in Fig. 5(a). This result is for probe light at an angle of incidence of 45 degrees, and the Al film is assumed to have a thickness of 130 Å.

To calculate $\Delta R(t)$ we then need the time- and space-varying elastic stress in the Al film due to the returning echo. This is a problem in elasticity theory somewhat similar to the problems treated in Refs. 37 and 38. The initial condition is a uniform thermal stress set up in the Al by the pump pulse. The shape of the strain pulse that is launched into the SiO_2 film is affected by the acoustic mismatch between the Al and the SiO_2, and this mismatch also produces further reflections of the returning echo inside the Al. In addition, we have corrected the pulse shape by including the effect of acoustic attenuation in the SiO_2 film. To do this we took the Fourier transform of the predicted pulse shape, and then multiplied each Fourier component by a factor $\exp[-2\alpha(\omega)d_s]$, where d_s is the thickness of the SiO_2 sample and $\alpha(\omega)$ is the experimentally measured attenuation at frequency ω. The modified spectrum was then transformed back to the time domain, and the final result for the echo shape was shown in Fig. 5(b). The absolute magnitude of the experimental $\Delta R(t)$ is not reliably known, and so the data have been multiplied by a scale factor to get a good fit to the theory.

---

[1]For a review see articles in *Amorphous Solids: Low Temperature Properties,* edited by W. A. Phillips (Springer, Berlin, 1981).

[2]This term is several times larger than the T^3 term expected from low-energy phonons according to the Debye theory.

[3]See, for example, S. Hunklinger and M. von Schickfus, in *Amorphous Solids: Low Temperature Properties* (Ref. 1).

[4]For the distinctions between the TLS model and the tunneling model, see W. A. Phillips, in *Amorphous Solids: Low Temperature Properties* (Ref. 1).

[5]W. A. Phillips, J. Low Temp. Phys. **7**, 351 (1972).

[6]P. W. Anderson, B. I. Halperin, and C. M. Varma, Philos. Mag. **25**, 1 (1972).

[7]For a survey, see S. Hunklinger, Philos. Mag. B **56**, 199 (1987).

[8]Equation (1) could be made more general, for example, by including the possible variation of v on ω, and the dependence of Λ and ν on the polarization of phonons.

[9]M. P. Zaitlin and A. C. Anderson, Phys. Rev. B **12**, 4475 (1975). See also the recent discussion by M. S. Love and A. C. Anderson, *ibid.* **42**, 1845 (1990).

[10]This fit is taken from J. E. Graebner, B. Golding, and L. C. Allen, Phys. Rev. B **34**, 5696 (1986).
[11]W. Dietsche and H. Kinder, Phys. Rev. Lett. **43**, 1413 (1979).
[12]J. Wolter and R. E. Horstman, Solid State Commun. **37**, 171 (1981).
[13]O. Koblinger, J. Mebert, E. Dittrich, S. Dottinger,W. Eisenmenger, P. V. Chantes, and L. Ley, Phys. Rev. B **35**, 9372 (1987).
[14]A. R. Long, A. F. Cattell, and A. M. MacLeod, J. Phys. C **19**, 467 (1986). This paper also includes a discussion of the earlier experiments of A. R. Long, A. C. Hanna, and A. M. MacLeod [J. Non-Cryst. Solids **35-36**, 1149 (1980)].
[15]J. Mebert, B. Maile, and W. Eisenmenger, In *PHONONS 89,* edited by S. Hunklinger, W. Ludwig, and G. Weiss (World Scientific, Singapore, 1990), p. 495.
[16]M. Rothenfusser, W. Dietsche, and H. Kinder, Phys. Rev. B **27**, 5196 (1983); in *Phonon Scattering in Condensed Matter,* edited by W. Eisenmenger, K. Lassmann, and S. Dottinger (Springer, Berlin, 1984), p. 419.
[17]R. Vacher, J. Pelous, F. Plicque, and A. Zarembowitch, J. Non-Cryst. Solids **45**, 397 (1981).
[18]H. J. Maris, C. Thomsen, and J. Tauc, in *Phonon Scattering in Condensed Matter,* edited by A. C. Anderson and J. P. Wolfe (Springer, Berlin, 1986), p. 374.
[19]C. D. Zhu, H. J. Maris, and J. Tauc, in *PHONONS 89,* edited by S. Hunklinger, W. Ludwig, and G. Weiss (World Scientific, Singapore, 1990), p. 498.
[20]Model 3800 Nd:YAG laser and Model 3500 dye laser from Spectra-Physics Inc., Mountain View, California.
[21]For a detailed description of the CVD process, see N. Goldsmith and W. Kern [RCA Rev. **28**, 153, (1967)]. For a comparison of physical and structure properties between bulk and CVD film, see M. Huffman and A. Navrotsky, J. Electrochem. Soc. **13**, 164 (1986); M. Huffman and P. McMillan, J. Non-Cryst. Solids, **76**, 369 (1985).
[22]H. R. Phillip, in *Handbook of Optical Constants of Solids,* edited by A. D. Palik (Academic, Orlando, 1985), p. 749.
[23]Supplied by Metal Crystals and Oxides, Cambridge, England.
[24]This was done with the Minimet electro-mechanical polisher from Buehler Ltd., Lake Bluff, Illinois.
[25]*Handbook of Chemistry and Physics,* edited by R. C. Weast (CRC, Cleveland, 1975)
[26]A. Pippard, Philos. Mag. **46**, 1104 (1955).
[27]K. S. Gilroy and W. A. Phillips, Philos. Mag. B **32**, 202 (1980), and references therein.
[28]R. Vacher and J. Pelous, Phys. Rev. B **14**, 823 (1976).
[29]R. Nava, J. Non-Cryst. Solids **76**, 413 (1985).
[30]O. L. Anderson and H. E. Bömmel, J. Am. Ceram. Soc. **38**, 125 (1955).
[31]R. E. Strakna and H. T. Savage, J. Appl. Phys. **35**, 1445 (1964).
[32]C. K. Jones, P. G. Klemens, and J. A. Rayne, Phys. Lett. **8**, 31 (1964).
[33]U. Strom, in *Far-Infrared Science and Technology,* Vol. 666 of *Proceedings of SPIE,* edited by J. R. Izatt (SPIE–The International Society for Optical Engineering, Bellingham, WA, 1986), p. 140.
[34]U. Strom (private communication).
[35]See, for example, L. D. Landau and E. M. Lifshitz, *Electrodynamics of Continuous Media* (Pergamon, New York, 1966), p. 272-279.
[36]D. Y. Smith, E. Shiles, and M. Inokuti, in *Handbook of Optical Constants of Solids,* edited by A. D. Palik (Academic, Orlando, 1985), p. 369.
[37]C. Thomsen, H. T. Grahn, H. J. Maris, and J. Tauc, Phys. Rev. B **34**, 4129 (1986).
[38]H. N. Lin, R. Stoner, H. J. Maris, and J. Tauc, J. Appl. Phys. **69**, 3816 (1991).